DOI: 10.1002/cmdc.200600314

# Ensemble-Docking Approach on BACE-1: Pharmacophore Perception and Guidelines for Drug Design

Vittorio Limongelli,[a] Luciana Marinelli,*[a] Sandro Cosconati,[a] Hannes A. Braun,[b] Boris Schmidt,[b] and Ettore Novellino[a]

*β-Secretase (BACE-1), a key enzyme in the etiopathogenesis and progression of Alzheimer Disease, is the focus of medicinal chemistry efforts both in the pharmaceutical industry and in academia. Despite the availability of diverse peptidomimetic BACE-1 inhibitors, nonpeptidic compounds suitable for oral delivery and transport across the blood brain barrier are in great demand. Herein, a number of active and structurally diverse inhibitors were selected and subjected to an ensemble-docking process into five BACE-1 X-ray structures. The calculated bioactive conformations of these inhibitors allowed us to build an exhaustive pharmacophore model, which captures both the common geometric and electronic features essential for enzyme inhibition. The model is intended to aid the rational design of new BACE-1 inhibitors. Furthermore, a comparison of BACE/cathepsin D X-ray structures was made to provide guidelines for the design of BACE-selective inhibitors.*

## Introduction

Alzheimer disease (AD) is a cerebral neurodegenerative pathology that is characterized by the progressive formation of insoluble amyloid plaques and fibrillary tangles.[1] Although AD is the most common cause of dementia in western industrialized countries, up to now, there is no approved causal treatment. The available symptomatic treatments or disease modifiers provide only limited benefits to the affected people. The approved drugs, such as vitamin E or AChE inhibitors, slow down but do not stop the disease progression.[2] Thus, a growing need exists for new effective therapies with a specific mode of action which allows control of the onset and the progression of the disease. Over the last decade, much attention has been paid to the cascade of physiological events that contribute or accompany AD.[3–5] It is generally accepted that, the β-amyloid precursor protein (APP) is cleaved by two proteases to generate the 40/42 amino acids long amyloid-β peptides (Aβ). The increased Aβ formation results in extracellular amyloid plaque deposition and it is accompanied by the intracellular formation of neurofibrillary tangles in the brain.[5,6] The neurotoxicity associated with the Aβ oligomerization is thought to cause neuronal death, brain inflammation, and finally AD.[7] The APP is processed by the major α- or the minor β-secretase pathway; the latter produces fragments which are further processed by γ-secretase.[8] In contrast to the nonpathogenic products of α-secretase, the β-secretase pathway produces pathogenic Aβ peptides. After the demonstration that β-secretase (BACE-1), a member of the pepsin family of aspartyl proteases, is the rate-limiting enzyme in the production of Aβ[9] and that its genetic depletion in mice abolishes the β-amyloid formation without major side effects,[10] BACE-1 has emerged as a leading target for the therapeutic treatment of Alzheimer disease.[11] Recently, BACE-1 was shown to control the myelination of the peripheral nerves in the late fetal development, the relevance of this finding to chronic treatment of adults will have to be considered.[12]

To date, several X-ray structures of BACE-1 (hereinafter referred to as BACE) have been reported, either in the apo form (PDB codes: 1SGZ and 1W50), in complex with large-size peptidomimetic ligands (1FKN, 1M4H, 1XN2, 1XN3, 1XS7, 2F3E, 1M2, 1M4, 2B8L, 2B8V, and 2FDP), or with rather small inhibitors (1W51, 1TQF, and 2G94). An important advance in the elucidation of the inhibitor–BACE recognition process has been provided by the 1W51 structure, where the enzyme has been cocrystallized with the inhibitor **1**.[13] Figure 1 highlights the main interactions between **1** and the BACE-1 enzyme.

A detailed comparison of the available X-ray structures suggests that BACE can assume at least two major conformations mainly differing in the FLAP region, which adopts an open and a closed conformation in the ligand free and ligand bound enzyme, respectively. Thanks to the availability of all these structures, great strides in the development of new BACE inhibitors have been made by both academic and industrial re-

[a] *Dr. V. Limongelli, Prof. Dr. L. Marinelli, Dr. S. Cosconati, Prof. Dr. E. Novellino*
*Dipartimento di Chimica Farmaceutica e Tossicologica*
*Università di Napoli "Federico II"*
*Via D. Montesano 49, 80131 Napoli (Italy)*
*Fax: (+39) 081 678139*
*E-mail: lmarinel@unina.it*

[b] *Dr. H. A. Braun, Prof. Dr. B. Schmidt*
*Clemens Schöpf-Institute of Chemistry and Biochemistry*
*Darmstadt University of Technology*
*Petersenstr. 22, 64287 Darmstadt (Germany)*

  

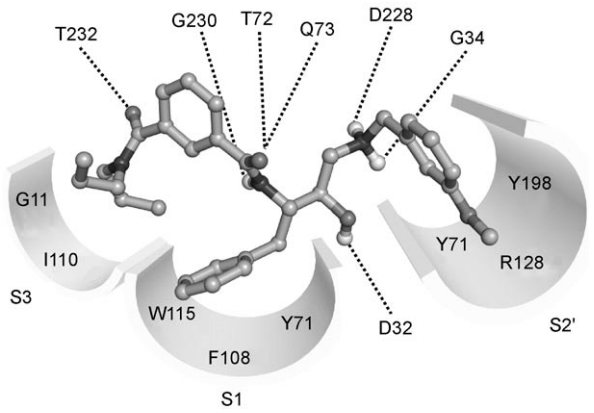


**Figure 1.** Schematic representation of the main interactions of **1** with the BACE catalytic site.

search groups. As a result, Vertex, and recently Wyeth, reported new inhibitors bound to BACE with the FLAP open conformation.[14]

Many noncleavable transition state isosters were designed as new inhibitors on the basis of initial kinetics and substrate specificity data.[15] Most of these peptide analogues mimic the scissile amide bond of the endogenous substrates.[16,17] The hydroxyethylene derivates, such as OM99-2 and OM00-3, represented the first class of highly potent BACE inhibitors.[15] The employment of the statine moiety led to the peptidomimetic compound **2** ($IC_{50}=20$ nM), which features nonpeptidic portions at both the C and N termini.[19] In an effort to reduce the peptidic character of the first inhibitors, several hydroxyethylamine-containing compounds were investigated as new BACE inhibitors. Among them, inhibitors **3** and **4** are of particular interest for their low nanomolar activity ($IC_{50}=1$ and 1.4 nM, respectively) and for the originality of their structures (the secondary amine of HEA is arranged in a six-membered cycle).[20] With the aim of achieving selectivity for BACE over the other aspartic proteases, a sulfonylamide group has been introduced in an HEA derivative leading to compound **6**.[21] Recently, BACE-1 selective compounds, (for example, compound **5**, $IC_{50}=4$ nM), featuring a $\Psi(CH_2NH)$ reduced amide bond were reported by Coburn et al.[22]

Despite this considerable progress, it is worth noting that the majority of the reported peptidomimetics with low nanomolar activity in BACE-1 enzymatic assays are poorly active in cell-based assays because of the limited cell membrane penetration. Thus, nonpeptidic inhibitors with a lower molecular weight suitable for oral delivery and transport through cell membranes and the blood-brain barrier are still in great demand. In spite of all efforts made by the pharmaceutical companies and academic groups, nonpeptidic leads for BACE inhibition are still few.[23] Thus, BACE is a structurally challenging target having on one hand multiple sites for effective binding and, on the other hand, a high homology with other aspartyl proteases such as cathepsin D, pepsin, or renin. Currently, medicinal chemists can choose among a number of novel approaches for drug discovery such as high-throughput in vitro screening, combinatorial chemistry, focused library or pharmacophore-based and/or target structure-based virtual screening (VS), the latter two approaches being increasingly used as they avoid long and expensive experimental efforts. However, the pharmacophore-based VS is exclusively possible when a trustworthy pharmacophore model exists, whereas the structure-based VS needs the design of a proper protocol as it is well-known that several features, such as the charge state of potential-interactive residues, the protein conformations (apo and ligand bound), the docking methods, and the scoring functions can all affect the success rate. In this regard, the works of Polgàr and Keserü[24] are particularly helpful, as the influence of protonation state of catalytic Asp residues of BACE (D32 and D228) and the enzyme conformations were investigated in a comparative VS. From these studies, it emerges that the monoprotonated form ($D228^-$, D32) of the BACE catalytic site gave a better enrichment factor compared to the default protonation state (D32 and D228 deprotonated), and ligands can find proper poses easier in a ligand-bound structure (FLAP closed), than in the unbound form (FLAP open). Interestingly, the introduction of pharmacophore constraints in the docking calculations improved enrichment factors for both structures (bound and unbound), reducing false positive ligand poses and increasing the inactive drop-out rate.

In structure-based VS, a 3D pharmacophore model can be used to constrict the number of the possible ligands poses or to prescreen compound databases, both helping to pursue a more accurate and time-saving simulations. The pharmacophore constraints used in the study of Polgàr and Keserü were retrieved from a patent document, in which a congeneric series of BACE-1 inhibitors were presented.[14]

Herein, with the aim of extending our understanding of inhibitor binding at the BACE-1 catalytic site and to provide an exhaustive structure-based pharmacophore model, the most active and selective (whenever possible) compound for each class of BACE inhibitor (**2**–**6**) was selected and subjected to an ensemble molecular docking process into five BACE X-ray structures. The superimposition of the calculated bioactive conformations of these inhibitors allowed us to capture both the common geometric and electronic features essential for the ligand recognition and the enzyme inhibition. Furthermore, to achieve BACE-1 selective inhibition, a comparison of the X-ray structures of BACE-1 and cathepsin D was made to better understand the structural and chemical differences in their respective catalytic sites.

The elucidation of the different binding modes of the diverse ligands on one hand, and the development of a pharmacophore model on the other, are intended to extend our knowledge of BACE furnishing support for pharmacophore- and/or structure-based VS techniques and a source for the optimization of the screened compounds and known leads. Moreover, the proposed pharmacophore hypothesis can be of help in the common target-based and ligand-based drug design approaches and for the construction of a focused-library of BACE inhibitors.

  

## Results and Discussion

### X-ray Structures Selection for the Ensemble Docking Studies.

Even today, a major hurdle for a successful molecular docking is protein flexibility. At present, many effective methods are available for docking a flexible ligand into a rigid protein, whereas docking calculations including target flexibility still remain problematic, both in terms of computational time and efficiency. In this respect, BACE shows the type of flexibility that can pose challenging problems in docking simulations as the enzyme is known to undergo a massive rearrangement of the FLAP region (residues 68–74) during association with ligands and a certain mobility is expected for the 10S loop (residues 9–14). To the best of our knowledge, no docking program that attempts to include wide protein flexibility has been extensively validated. Fortunately, in the case of BACE, numerous crystallographic structures exist enabling us to use an ensemble of enzyme conformations for our docking calculations. Although far from being perfect, docking a ligand into a battery of binding pockets is a strategy to deal with the protein flexibility.

A comparative structural analysis of all available BACE structures revealed that the FLAP region is always in the closed conformation whenever an inhibitor, either peptidomimetic or nonpeptidomimetic, is bound. As ligands **1**–**6** are substrate analogues that interact with the FLAP-closed form of BACE, we limited our studies to all BACE structures with a FLAP closed conformation (PDB codes: 1FKN, 1M4H, 1TQF, 1XN2, 1XN3, 1XS7, 1M2, 1M4, 2B8L, 2B8V, 2FDP, 2G94, 2F3E, and 2F3F). With the aim of reducing the BACE structure redundancy, only the most divergent structures were considered for our docking calculations.

To assess the differences among the BACE structures, they were superimposed on the alpha carbon atoms (Cα) using 1W51 as a reference structure. Interestingly, the FLAP closed conformations are all surprisingly similar regardless of the inhibitor type bound, whereas some differences emerged in the side chain conformations of a few residues, with the most notable one residing in Q73 (Figure 2). Additionally, some expected flexibility was also found in various residues lining the binding site cleft such as R128, T231, R307, and R235.

From the comparative analysis of BACE X-ray structures, it is clear that the 10S loop, a short loop located between two strands at the base of the S3 subpocket, displays three main low-energy conformations, an open (1FKN, 1XN3, 1XN2, 1XS7, 1M2, 1M4H, 2F3F, and 2G94), a closed (1W51, 1FDP, 2B8L, 2B8V, 1M4, and 2F3E), and an outlier conformation (1TQF) (Figure 2).

In view of the capability of the 10S loop to affect the shape of the S3 subpocket (S3 sp) and thus ligand binding,[25] the inclusion of such structural variability in a docking study becomes of fundamental importance. Consequently, 1FKN,[26] 1W51,[13] and 1TQF,[27] were chosen for our docking experiments as they cover the experimentally observed motions of the 10S loop and of some residues in the catalytic site such as Q73, R128, R307, R235, and T231. Two additional structures were considered (1XN3 and 2G94)[28,29] so as to include additional conformers of Q73 and R235 residues. As a result, each ligand was docked in a total of five BACE structures (1FKN, 1W51,1TQF, 2G94, and 1XN3).

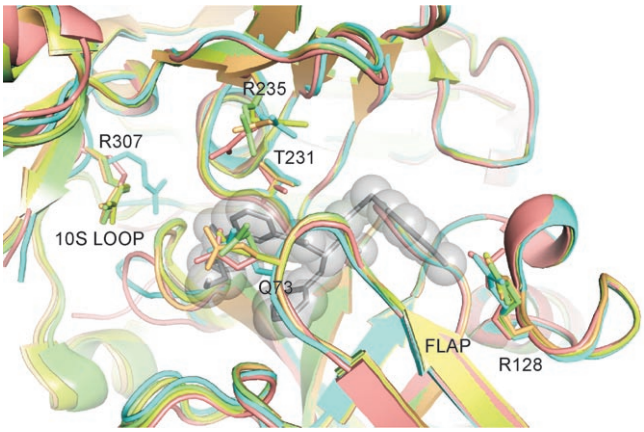


**Figure 2.** Cartoon representation of the BACE X-ray structures used for the ensemble-docking study (1W51, 1FKN, 1TQF, 1XN3, and 2G94 are in pink, green, cyan, yellow, and orange, respectively) with **1** shown as gray sticks and transparent grey spheres; hydrogen atoms are omitted for reasons of clarity. The most flexible residues, emerged from the BACE X-ray structures superposition, are represented in stick mode and colored according to the BACE structures color code.

### Assessment of the Docking Program.

Although AutoDock program is the most widely used docking program[30] and has been extensively validated, it is well known that each docking algorithm performs better for certain protein systems than for others, thus the reliability of a docking program for the target of interest has always to be assessed. Furthermore, testing a program by docking a ligand into its native protein is intrinsically biased because the protein has already changed its shape to better accommodate the ligand and this unavoidably positively affects the docking results. Herein, with the aim to accurately evaluate the program performances on the studied system, a cross-docking experiment of **1** in its native enzyme (1W51) and in four non-native enzyme conformations (1FKN,1TQF, 2G94, and 1XN3) was conducted. It is generally accepted that a successful docking result reproduces the crystallographic conformation of a ligand in the complex structure within ~2 Å of RMSD on all ligand atoms, and that the first-ranked docked conformation (herein referred as ranking conformation) is the preferable one. On the other hand, our experience indicates that the lowest energy conformation of the most populated cluster (herein referred as cluster conformation) has to be taken into account when using the AutoDock program. In the case of BACE in two complexes (1W51 and 2G94), the conformation calculated by AutoDock with the lowest free energy of binding belongs to the most populated cluster, thus, no ambiguity exists for the selection of the best binding pose. The AutoDock program reproduced the experimental binding mode of **1** (Figure 2) both in the native

  

(1W51) and non-native (2G94) enzyme structure, with RMSD values of 0.4 and 0.6 Å, respectively. For the other three enzyme structures, good results were obtained considering the cluster conformations (0.59 Å for both 1FKN and 1TQF, and 1.20 Å for 1XN3) whereas the accuracy in reproducing the X-ray conformation lowered when the ranking conformation was considered only (2.9 Å for 1FKN, 3.4 Å for 1TQF and 2.8 Å for 1XN3).

To make the test independent of the single ligand used (**1**), we carried out an additional cross-docking experiment using the inhibitor referred to as compound **5** in the paper of Ghosh et al. (complex PDB code: 2G94).[28] The experimental binding conformation of the Ghosh ligand was well reproduced in four out of five BACE structures when either the ranking or the cluster conformation is considered. Specifically, in 1TQF and in the native 2G94 BACE structures, AutoDock perfectly predicted the experimental pose (RMSD value of 1.45 and 1.12 Å, respectively) and provided one unambiguous solution as the ranking conformation belongs to the most populated cluster. In 1FKN and 1W51 structures, the ranking conformation reproduces the correct pose with an RMDS value of 1.82 and 1.46 Å, respectively. AutoDock did not reproduce exactly the X-ray conformation of the inhibitor in the case of 1XN3 (RMSD value of 3.10 Å). After a visual inspection of the docking results, it was clear that the cluster conformation places the ligand in a very similar way to the X-ray conformation apart from the diazole branch that fills the S2 region replacing the sulfonyl moiety. This exchange might be due to the different conformation of Arg 235 in the 1XN3 structure with respect to the other X-ray BACE structures. All in all, our test experiments clearly prove that the AutoDock program can be successfully applied to the BACE-1 field, although whenever the ranking conformation does not correspond to the cluster, both solutions have to be taken in consideration. The final choice between the ranking and the cluster conformations will be governed by their coherency with available experimental data (for example SAR).

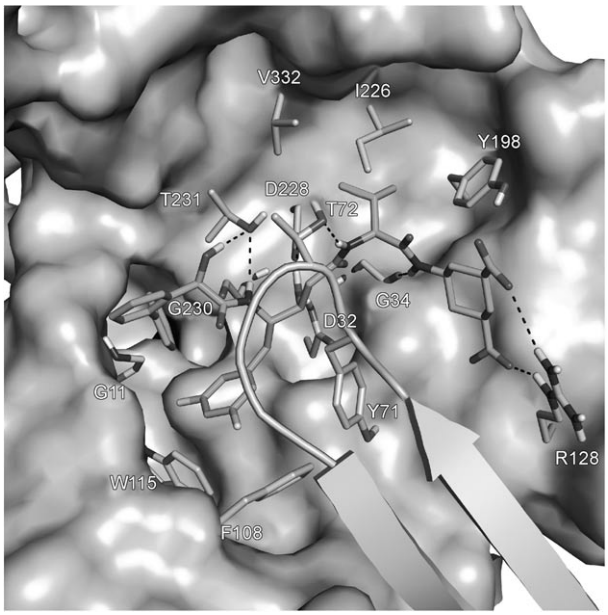


**Figure 3.** Binding mode of compound **2** into the BACE catalytic site represented as Connolly surface. The ligand and the interacting residues are shown in stick representation and shaded by atom type, whereas the FLAP region is represented by a cartoon. Hydrogen bonds are represented with dashed black lines. All nonpolar hydrogens were removed for clarity.

**Docking Results.**

*Docking of* ***2****.* As a result of the undetermined absolute stereochemistry of the carbon atom attached to the biphenyl ring of compound **2**,[19] both stereoisomers were subjected to docking calculations.

Docking of **2** with the (*R*) absolute stereochemistry revealed that in four out of five calculations (1TQF, 1W51, 1XN3, and 2G94) comparable results were found for all the predicted ranking conformations. Using 1FKN as receptor, docking of **2** did not succeed in predicting a plausible binding mode, therefore it was omitted from the comparison. As depicted in Figure 3, the (*S*) statine isoster places the hydroxyl group in between the catalytic dyad allowing simultaneous interaction with D32 and D228 as previously observed in other X-ray complexes (for example, 1FKN).

The difluorobenzyl moiety of **2** (P1) occupies the aromatic pocket S1, analogous to the corresponding benzyl group of **1**. Notably, because of the withdrawing property of the fluorine atoms present on the aromatic system of **2**, the charge transfer interactions of the P1 branch in **2** with the Y71, W108, and P115 aromatic rings are expected to be stronger with respect to those observed for compound **1**. Similarly to **1**, the calculated binding mode preserves the H-bond with G34 backbone CO, whereas two additional H-bonds with T72 and T231 side chains are present (Figure 3).

Unfortunately, a direct comparison between the potency of **2** ($IC_{50}=20$ nM) and **1** ($IC_{50}=200$ nM) is not meaningful because of the different biological assays. In contrast to **1**, compound **2** features an isopropyl group (P1′) which establishes hydrophobic contacts with the I226 and V332 side chains (S1′ pocket) whereas the biphenyl moiety deepens into a narrow passage (S3 sp) formed mainly by two glycines (G13 and G230). An interesting feature of **2**, which certainly contributes to its great potency ($IC_{50}=20$ nM), is the aminocyclohexanedicarboxylate moiety (P2′), which was inserted to mimic the C-termini of the first known peptidic inhibitors.[15,18] Indeed, docking results confirm that this P2′ moiety entirely fills the S2′ hydrophobic pocket with both the carboxylate groups engaging a charged-reinforced H-bond with the guanidine group of R128.

Docking of **2** with the biphenyl unit attached in the (*S*) configuration gave a slightly different binding conformation in comparison to that found for the (*R*) isomer for three out of the five docking calculations (1FKN, 1XN3, and 2G94). Indeed, the main interactions with the enzyme are well conserved for this isomer whereas some differences are observed for the N-terminal moiety (P3 branch). Here, the biphenyl group points into the S3 sp, similar to the (*R*) isomer, whereas the hydroxyl function due to its (*S*) stereochemistry is now incapable of interacting with T231. Although it is not known which is the

  

most active diastereoisomer, it has been reported that one isomer is 100-fold more active than the other.[19] Our docking results do not clearly discriminate between the two analyzed isomers. Nevertheless, the low convergence of docking results for the (*S*) isomer allows us to hypothesize a weaker binding to BACE if compared to the (*R*) isomer.

However, the proposed binding modes are in alignment with the available SAR data.[19] Indeed, analogues of **2** featuring nonacidic aminocyclohexanedicarboxylate derivatives do not interact with R128, this results in a loss of activity.[19]

Furthermore, the replacement of the aminocyclohexanedicarboxylic moiety by 4-aminomethylbenzoic acid, presenting only one acidic function, caused a tenfold loss of activity thus demonstrating the contribution of both acidic groups to enzyme binding. Interestingly, the aminocyclohexanedicarboxylic methylester derivative displays only a tenfold decrease in inhibitory activity. These data are in accordance with our results, which place the aminocyclohexanedicarboxylic near to R128, where the carbonyl of the methyl ester forms an H-bond with the guanidine side chain.

*Docking of **3** and **4**.* The binding pose of **3** does not substantially change when different enzyme structures are used and basically resembles the binding position found for **1** and **2**. As depicted in Figure 4a, the hydroxyl group of the HEA core H-bonds with D32, whereas the protonated secondary amine, which differs from **1** by the locked conformation of the 6-membered ring, engages a salt bridge with D228 and H-bonds with G34. Interestingly, all HEA derivatives feature an unusual stereochemistry at the secondary alcohol (R absolute configuration). A secondary amine in the HEA derivatives causes the interaction with D228, which would be lost by the inversion of the stereochemistry at the secondary alcohol. The benzyl ring (P2′) is stacked in between the Y198 and Y71 residues (S2′ pocket), whereas the ligand amide group H-bonds with G230 and Q73. Analogous to **2**, the difluorobenzyl branch (P1) fills the S1 pocket shaped by the Y71, F108, and W115 residues (Figure 4a).

Whereas the above-described interactions are conserved in all five BACE structures, an ambiguity was encountered for the relative position of the imidazolidinone moiety. Ligand docking into 1W51 and 1XN3 structures placed the imidazolidinone so as to allow the carbonyl group to H-bond with the T232 backbone, the benzyl group (P2) to establish a cation-π interaction with the guanidine group of R235, and the *N*-alkyl substituent to thread into the narrow S3 subpocket (S3 sp) (Figure 4a). However, the ligand docking into the 1FKN and 1TQF structures, placed the imidazolidinone ring so that the phenyl ring pointed to the S3 sp, whereas the alkyl chain pointed out of the enzyme. In this case, ensemble docking leads to two comparable but not equal conformations. A subsequent analysis of BACE structures suggests that the different conformations of the R235 side chain are mainly responsible for the divergent results. More precisely, in 1W51 and 1XN3 the R235 side chain is optimally oriented to engage a cation-π interaction with the phenyl ring of **3** (Figure 4a), whereas in 1FKN and 1TQF the R235 guanidine group partially occludes the catalytic site so as to prevent the placement of the phenyl group. Although both ligand conformations are feasible, the orientation of the N-alkyl substituent into the S3 sp and the benzyl moiety towards the external part of the enzyme maximizes the interaction with the protein by allowing the formation of a H-bond with T232 and a cation-π interaction with R235. Further support for this hypothesis is provided by recent X-ray studies outlining the importance of the interactions with T232 and R235.[31]

Similar to **3**, the HEA isoster in **4** interacts well with both the catalytic aspartates and with G34 (Figure 4b). The benzyl and difluorobenzyl moieties of the ligand optimally fill the S2′ and the S1 pockets, respectively, whereas the isophthalamide group lies in the S2 open region with one of the two amide functions H-bonding with G230 and Q73. Interestingly, the

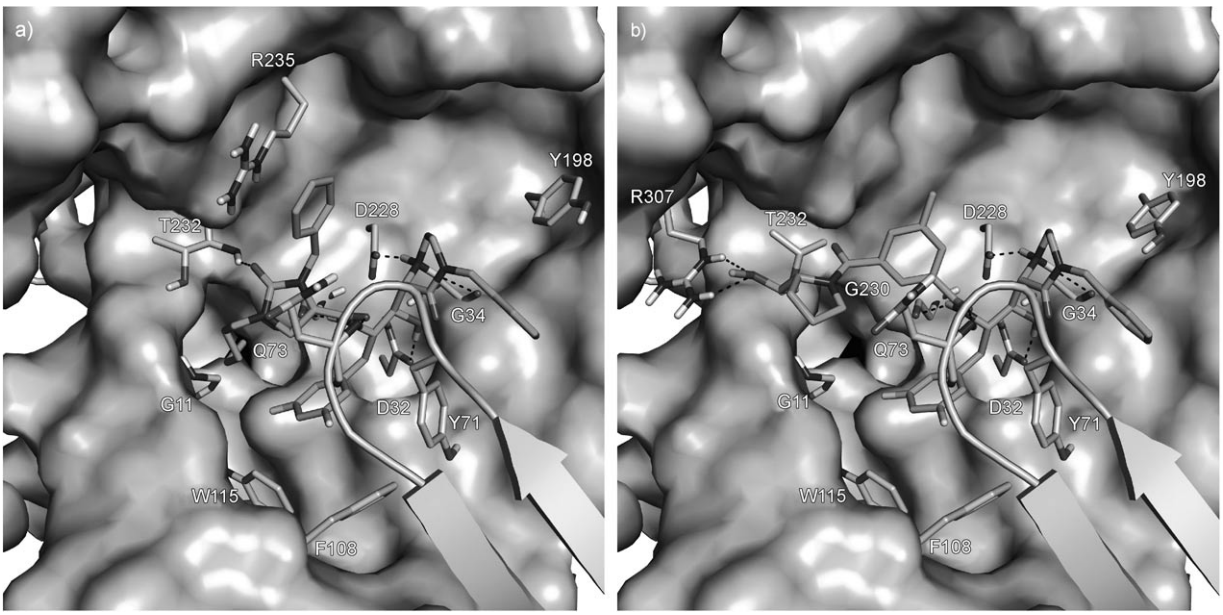


**Figure 4.** Binding modes of compound **3** (a) and **4** (b) into BACE catalytic site.

  

methoxymethyl substituent of the pyrrolidine protrudes above the S3 sp, where polar interactions occur with the R307 and T232 side chains. The high potencies of **3** and **4** ($IC_{50}=1$ nM, $IC_{50}=1.4$ nM, respectively) suggest that T232, R235, and R307 are further points of ligand attachment, strengthening the inhibitor binding.

*Docking of **5** and **6**.* Ensemble docking experiments on both **5** and **6** showed convergence of results. In fact, all the docking calculations apart from one (1W51) detected a single solution which is both the ranking and cluster conformation.

The protonated nitrogen of **5** was found to interact with D228 whereas the isobutylamide branch (P2′) engages H-bonds with T72 and G34 placing the alkyl chain into the hydrophobic S2′ pocket (Figure 5a). The *n*-propyl branch (P1′) lies in the S1′ pocket shaped by hydrophobic amino acids such as I226, V332, and Y198. The benzyl group (P1) is placed into the aromatic cage S1 with the adjacent amide group forming two H-bonds with G230 and Q73. Comparing the binding modes of the docked ligands, we noticed that H-bonds with G230, T72, or Q73 backbones are frequently present and this seems to be important for high BACE inhibitory activity.[32] Interestingly, in all the five BACE structures used for the ensemble docking, the *N*-methyl methylsulfonamide group (P2) was found in a polar region among N233, S325, and R235, mostly interacting with the latter residue. The proposed location of the sulfonamide function is in line with the recently reported X-ray structures of BACE complexed with some sulfonamide-containing ligands.[21,27,29,32]

The difluorobenzyl branch deepens inside the narrow channel in the S3 sp engaging a T-shape interaction with Tyr 14 (Figure 5a). It is interesting to note that this channel constitutes the access to an additional small pocket lined by hydrophobic residues (L152, L154, V31, and Y14) and to date no inhibitor has entirely filled this newly identified pocket.

The hydrophobic interactions of the *n*-propyl branch (P1′) in the S1′ pocket are supported by SAR data which show a slight decrease of activity for the ethyl and/or methyl (P1′) substituent.[22] Furthermore, additional SARs suggest that a H-bond donor on the P2′ substituent can be important for BACE activity and this is in agreement with our finding of an H-bond interaction between the isobutylamide branch and the G34 backbone.

Compound **6** docked in a mode similar to **5**. Nevertheless, **6** being a HEA derivate, it contacts both D32 and D228, as described for all the other HEA derivates. Whereas the benzyl group (P1) deepens into the S1 pocket, the sulfonamide group engages an electrostatic interaction with R235 (Figure 5b).

The two cyclopropyl branches of **6** fit in the hydrophobic S1′ pocket and S3 sp, respectively. Despite the structural similarity, compounds **5** and **6** show different activities ($IC_{50}=4$ and 35 nM, respectively). According to our docking results, this difference in potency has to be ascribed to the additional interactions established by **5**, which occupies S3 sp, S1′, and S2′ pockets, whereas **6** just partially occupies the S3 sp and S1′ pockets and does not fill the S2′ pocket at all.

**Pharmacophore fingerprints and guidelines for drug design.**

The superimposition of the calculated bioactive conformations of inhibitors **1**–**6** (Figure 6a) allowed us to capture both the common geometric and electronic features essential for ligand recognition and the enzyme inhibition. From the analysis of the interactions established between the ligands and the enzyme, it is apparent that both polar and hydrophobic interactions are equally important in the inhibitor-enzyme recognition process.

Despite the structural diversity, compounds **1**–**6** are linked by five highly conserved pharmacophoric points (blue spheres

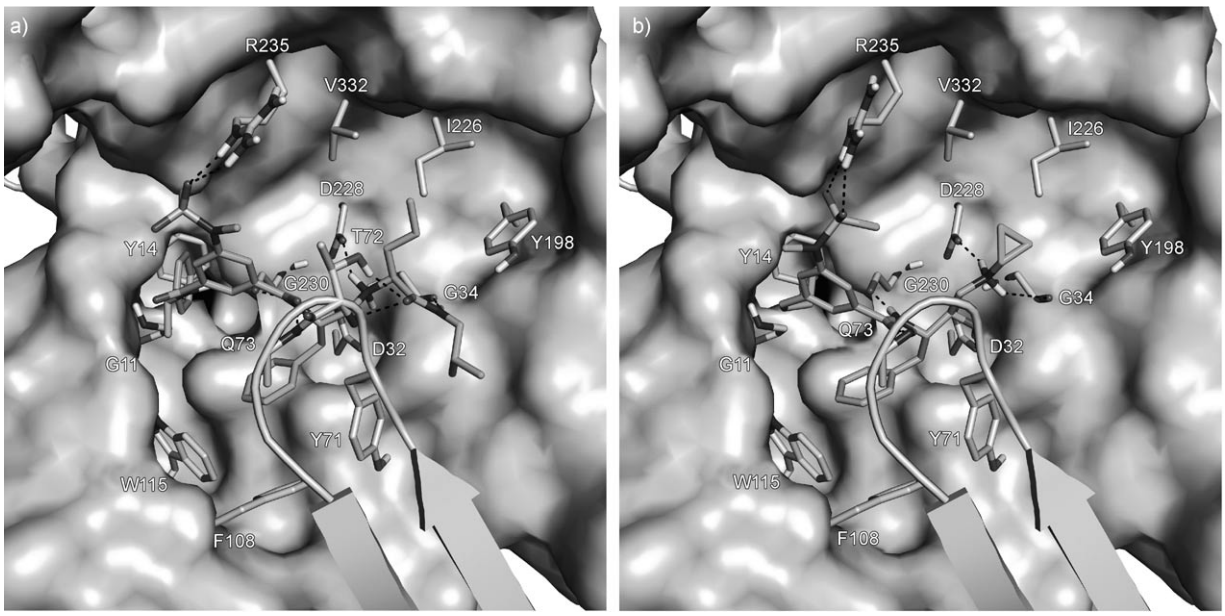


**Figure 5.** Binding modes of compound **5** (a) and **6** (b) into BACE catalytic site.

  

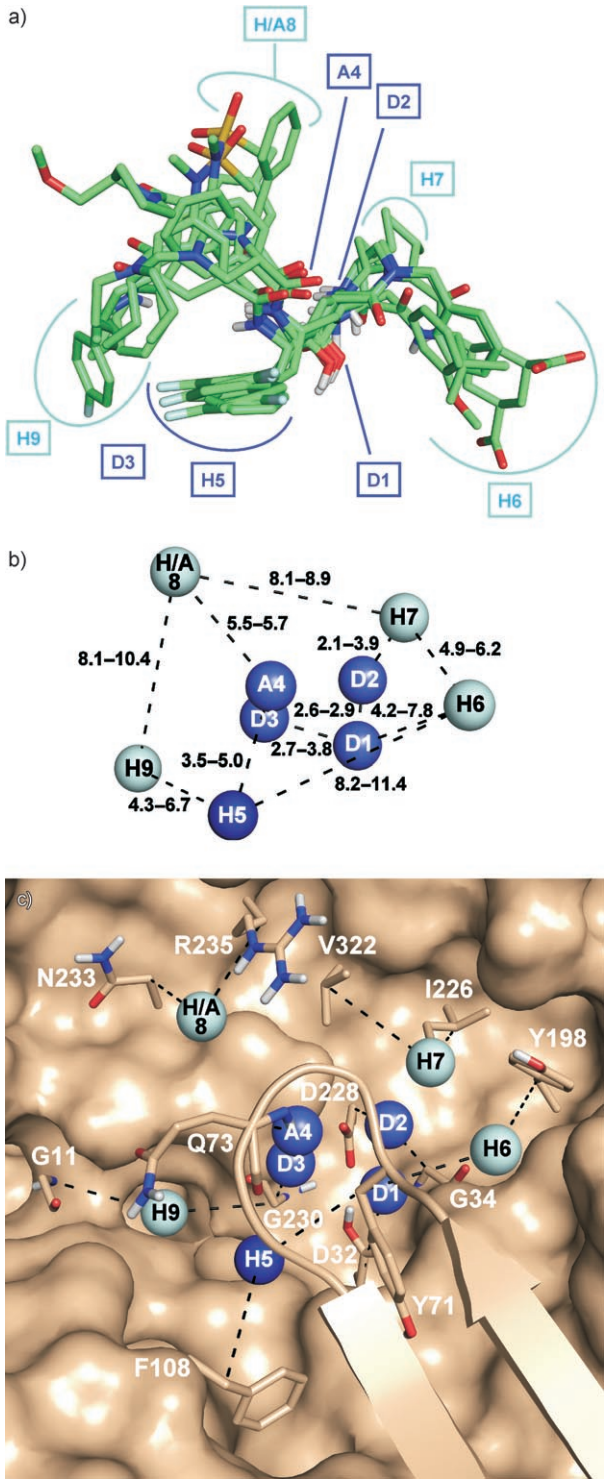


**Figure 6.** a) Overlay of bioactive conformations of compounds **1**–**6** on the experimentally determined bound conformation of **1**. The pharmacophoric points are color coded as conservative (blue) or additional (cyan). The nonpolar hydrogens are omitted for clarity. The letter "A" corresponds to an H-bond acceptor group, "D" to an H-bond donor, whereas "H" represents a hydrophobic group. "A/H" means that an H-bond acceptor or a hydrophobic group is tolerated. b) Three-dimensional representation of the distances between the identified pharmacophoric points. The distances are reported in Å and represent the minimum and the maximum values found in the proposed bioactive conformations of **1**–**6**. The distances were calculated considering the nitrogen and oxygen atoms of the H-bond acceptor and donor groups, the sulfur atom of the sulfonamide function, the centroids of the aromatic rings, and the center of mass of the alkyl and cycloalkyl groups. c) Mapping of the pharmacophoric points into the BACE catalytic site represented as Connolly surface. Interactions between the pharmacophoric points and some BACE residues are highlighted by black dashed lines.

in Figure 6b and c): three H-bond donors (D1, D2, and D3), one acceptor (A4), and one hydrophobic centre (H5). All compounds, with the exception of **5**, feature an interaction point with D32 (D1) and with the other catalytic aspartate (D228) through the D2 point. This observation confirms the importance of the interaction with the two binding site catalytic aspartates for effective enzyme inhibition. Furthermore, all compounds, apart from **2**, present the D2 point. This highlights the convenient insertion of a protonable amine in this position to achieve a simultaneous interaction with D228 and G34 residues. As shown in Figure 6c, the D3 point donates an H-bond to the G230 backbone CO whereas the H-bond acceptor A4 interacts with either T72 or Q73 backbone NHs. It is noteworthy how these two latter points (D3 and A4) represent an ancestral inheritance of the endogenous ligands of BACE where these points are normally filled by an amide moiety of the peptidic backbone.

Despite the relevance of such polar features, the hydrophobic point H5, constantly present in **1**–**6**, underlines the essential role of an hydrophobic group in this position, interacting with the S1 pocket residues Y71, W108, and F115. (Figure 6c).

The frequent occurrence of D1, D2, D3, A4, and H5 pharmacophoric points in the analyzed compound set (Table 1) suggests that these are the indispensable features for ligand recognition. Unfortunately these interactions do not offer the key to selective BACE inhibition, because of the conservation of the majority of their corresponding interacting residues in other proteases such as cathepsin D as discussed hereafter.

From our docking results, four additional pharmacophore points, represented as cyan spheres in Figure 6b and c, emerge. They are mostly hydrophobic (H6, H7, and H9), with the exception of one, that can be either hydrophobic or a polar (H/A8).

The H6 point represents a hydrophobic feature able to reach the S2′ pocket (Figure 5c). The structural variability of this feature (Figure 6a) demonstrates that, although an aromatic substituent in H6 is not mandatory (see compounds **2** and **5**), a hydrophobic group is required because of the nonpolar character of the S2′ pocket. It is worth noting that in all analyzed compounds, only **2** features the optimally functionalized H6 point having two carboxyl groups that establish a double salt bridge with R128. Such an interaction is particularly interesting as R128 is a unique feature of BACE enzyme. To achieve a better pharmacokinetic profile yet preserving good inhibitory potency, the acidic functions

  

**Table 1.** Pharmacophoric points present in ligands **1**–**6**.

| Compounds | Points |
|---|---|
| 1 | D1-D2-D3-A4-H5-H6-H9 |
| 2 | D1-H5-H6-H7-H9 |
| 3 | D1-D2-D3-A4-H5-H6-H/A8-H9 |
| 4 | D1-D2-D3-A4-H5-H6 |
| 5 | D2-D3-A4-H5-H6-H7-H/A8-H9 |
| 6 | D1-D2-D3-A4-H5-H7-H/A8-H9 |

present in the H6 point could be methylated without preventing the ability to H-bond with R128.

The additional point H7 finds space in the hydrophobic S1′ pocket (I226, V332, and Y198) where, because of its limited dimensions, only an alkyl or cycloalkyl chain with a maximum of three carbon atoms seems to be tolerated. This position was recently employed to achieve selective BACE inhibition and should be investigated further.[33]

Another pharmacophoric point, which may be exploited to achieve BACE-selectivity, is represented by the H/A8 point, which is located in the S2 open region and can be either hydrophobic or polar. An H-bond acceptor in this position, such as a sulfonamide (compounds **5** and **6**), or an hydrophobic phenyl ring (compound **3**) can interact with the surrounding residues such as N233, R235, and S325. These three residues are peculiar to BACE in comparison to other proteases, thus this interaction is expected to have an important role in the BACE selectivity. Our observation is in accordance with the recently reported X-ray analysis of the co-crystallized complexes of some selective BACE inhibitors featuring a sulfonamide group as H/A8 point.[27,29]

After the superposition of all compounds in their predicted binding poses, different sized branches at the H9 point indicate that aliphatic and aromatic branches are well tolerated in the S3 sp. The extension of this pocket mainly depends on the conformation of the 10S loop, but it has to be pointed out that among all analyzed compounds, only inhibitor **5** goes across the S3 sp, reaching with its aromatic system the inner hydrophobic pocket made by L152, L154, Vl31, and Y14 residues. This cavity should be further explored for the design of new BACE inhibitors, as demonstrated for the renin inhibitor aliskiren.[34] Comparing the BACE and renin cavities, we noticed that they have chemical and structural differences, which offer additional chances to improve the inhibitor selectivity.

The compounds **1**–**6** are characterized by five to eight identified pharmacophoric points (Table 1); appropriate chemical modifications can result in more potent analogues. For instance, the BACE binding affinity of compound **5** may be improved by the addition of an hydroxyl group on the carbon of the $\Psi(CH_2NH)$ reduced amide bond so as to present the D1 point and complete the nine-point pharmacophore.

Regarding compound **1**, the substitution of the *n*-propyl chain with a benzyl moiety may optimize the interactions with the BACE S3 sp and the addition of an H-bond acceptor in position 2 on the isophthalamide group, such as a sulfonate or carbonyl group, may provide the basis for BACE selectivity.

So far, only one pharmacophore model derived from a congeneric series of BACE inhibitors has been disclosed by a patent application by Vertex.[14] The authors proposed that the flap is shifted and stabilized in an open conformation in the presence of their inhibitors.

Comparing the Vertex pharmacophore model with ours, we found that the two models are rather similar regarding the pharmacophoric points interacting with the residues unaffected by the flap movement (Table 2). In particular, the Vertex model shares a pattern of three H-bond donors and two hydrophobic points corresponding to D1, D2, and D3, and H5 and H6 in our model. Despite the general coherency of the chemical features of these points in both pharmacophoric models, the reported distances between them diverge to a large extent. For instance, in our model, the distance between D1 and D2, and D1 and D3 is a maximum of 2.9 and 3.8 Å respectively, (see Figure 6b) whereas in the Vertex model both range from 4 to 5 Å. Moreover, the D1–H6 distance is calculated in the range of 4.2–7.8 Å in our pharmacophore model and this value is very low in comparison to the minimum distance of 8 Å reported for the corresponding points in the Vertex model (HB-1 and HPB-3, respectively). This discrepancy may be due to the fact that the Vertex model places the HPB-3 point in a different pocket of the S2′ region.

The discrepancies found between the two pharmacophoric models can be assigned to the different compounds used for model generation. The Vertex pharmacophore is derived from a congeneric series based on a piperazine scaffold which are thought to stabilize the flap in an open conformation. Consequently, in their pharmacophoric model, an additional hydro-

**Table 2.** Distances (Å) between the pharmacophoric points and the BACE interacting residues.

| Pharmacophoric Points | Interacting Residues | Distances[a] |
|---|---|---|
| D1 | D32 | 4.9 |
| D2 | G34 | 3.7 |
| | D228 | 4.5 |
| D3 | G230 | 4.4 |
| A4 | Q73 | 4.5 |
| H5 | Y71 | 5.4 |
| | P108 | 8.9 |
| H6 | Y71 | 5.4 |
| | Y198 | 8.1 |
| H7 | I226V332 | 6.0 |
| | | 6.4 |
| H/A8 | R235 | 5.6 |
| | N233 | 5.3 |
| H9 | G11 | 5.1 |
| | G230 | 4.5 |

[a] The distances were calculated considering the pharmacophoric points and each Cβ of the corresponding residues, Cα were taken into account for glycine residues. As pharmacophoric points the nitrogen and oxygen atoms of the H-bond acceptor and donor groups, the sulfur atom of the sulfonamide function, the centroids of the aromatic rings, and the center of mass of the alkyl and cycloalkyl groups, were considered.

  

phobic point referred as HPB-2 is involved in the interactions with the flap pocket (W76, F108, F109, W115, and I102). Here, we have used BACE with the flap in a closed conformation, thus this pocket is no longer present. Consequently the HPB-2 point has to be considered a typical feature of the open flap pharmacophore model.

With respect to the Vertex model, our model offers an accurate description of three new pharmacophoric points: A4, H7, and H9, which are particularly important for a selective BACE inhibition.

The structural diversity of the compounds used in our study contributes to the value of our pharmacophore model, which is also substantiated by the X-ray structure of the binding conformation of compound **1**, perfectly filling the seven pharmacophoric points.

The design of new BACE inhibitors has to consider the other human aspartic proteases which could be potentially inhibited by BACE ligands, such as renin, napsin A and B, cathepsin E, pepsinogen A and C, and cathepsin D. Indeed, the catalytic domain of BACE is similar to that of other aspartyl proteases and the interactions of these enzymes with their inhibitors do not diverge too much from those we observed in the case of BACE. For instance, most of the human aspartyl proteases accept a phenylalanine analogue in P1. The selectivity versus BACE over other human aspartic proteases is required to avoid adverse side effects and is thus mandatory for clinical development of BACE inhibitors. For instance, inhibition of cathepsin D, which is largely expressed in all cells and controls their protein catabolism,[35] would likely result in consummation of the BACE inhibitor and the occurrence of toxicity.

Therefore we performed a structure-based sequence alignment of BACE and cathepsin D to investigate the differences in their binding sites (Table 3). The superposition of BACE and cathepsin D three-dimensional structures reveals that the two enzymes display very similar residues in their binding sites and consequently possess a similar shape, which is visualized by their Connolly surfaces in Figure 7. In addition to the catalytic dyad, several residues important for the ligand recognition such as G34 or G230 (G35 and G233 in cathepsin D) are conserved. As shown in Figure 7, the shape of the hydrophobic S1 and S2′ pockets is equivalent in BACE and cathepsin D. However, a careful comparison of the two binding sites reveals several important points of diversification (Figure 7).

Probably the most striking difference is located near to the catalytic dyad and thus easily accessible to the inhibitors; it concerns the S2 pocket, which presents the polar triplet N233-R235-S325 in BACE and the hydrophobic triplet L236-V238-M307 in cathepsin D. In line with this observation, a series of highly selective inhibitors containing a sulfonyl group in the P2 branch interacts with the residues of the BACE S2 region.[27,29] Besides the different character of the S2 region in BACE and cathepsin D, the space available for the ligand binding in cathepsin D is limited by the M307 and M309 side chains; these are replaced by less spacious residues in BACE (S325 and S327). This finding suggests the incorporation of bulky P2 branches, functionalized with polar groups capable of interacting with the BACE triplet (N233-R235-S325).

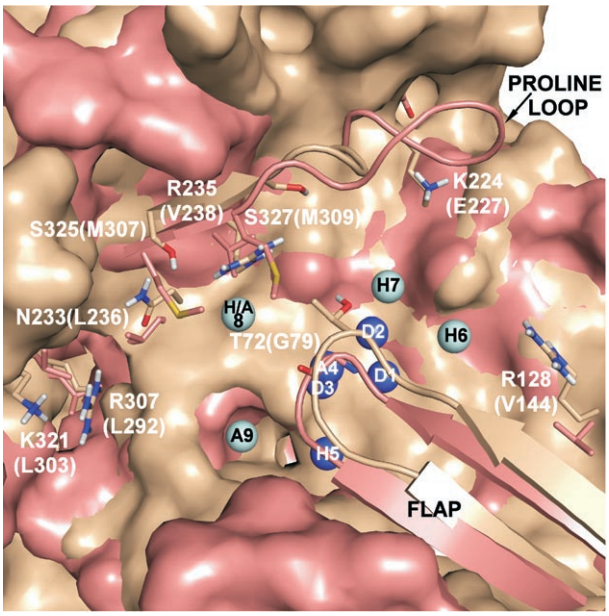


**Figure 7.** Superposition of BACE (pink) and cathepsin D (bown) structures represented as Connolly surfaces. The pharmacophoric points were mapped into the BACE enzyme. Mutated residues in the binding pocket are shown in stick representation and labeled with the one-letter amino acid code. The letters and the number in parentheses refer to the cathepsin D enzyme.

**Table 3.** Main dissimilarities in BACE and Cathepsin D catalytic sites.

| Binding Site Location | BACE residues | Cathepsin D residues |
|---|---|---|
| S2 Open Region | N233 | L236 |
| | R235 | V238 |
| | S325 | M307 |
| | S327 | M309 |
| S1′ pocket | K224 | E227 |
| Loop between S1′ and S2′ | S328, T329 and G330 | D310, I311, P312, P313, P314, S315, G316, P317, and L318 |
| S2′ pocket | R128 | V144 |
| Flap Region | T72 | G79 |
| Others | K321 | L303 |

The superposition of BACE and cathepsin D reveals significant differences in the length and sequence of the loop defining the S1′/S3′ pocket. Indeed, this loop is shorter in BACE (S327, S328, T329, and G330) than in cathepsin D, which presents a long loop of ten residues containing a rigid section called proline loop (P312, P313, P314, S315, G316, and P317).

This relevant difference indicates an alternative way to achieve BACE/cathepsin D selectivity. Indeed, a properly oriented bulky moiety on the P1′ substituent will occupy the BACE S1′ pocket and will not be tolerated by cathepsin D. Moreover, the mutation of BACE-K224 to E227 in cathepsin D, suggests the insertion of a hydrogen bond acceptor or a negatively charged group on the bulky moiety. To our knowledge, only few peptidic inhibitors targeted an interaction with K224.[15,18]

Another dissimilarity between BACE and cathepsin D resides in the S2′ pocket, where R128 is replaced by V144 in cathep-

  

sin D. Therefore, inhibitors including one or more acidic functions on the P2′ branch are expected to favor the interaction with BACE. The cathepsin D flap region, where G79 replaces the BACE-T72, offers another opportunity for enhancing the selectivity. The last divergence of BACE/cathepsin D resides in the region above the S3 pocket. Here, as shown in Figure 7, two basic amino acids (R307 and K321) are replaced by two hydrophobic residues (L292 and L303) in cathepsin D. Thus, compounds presenting an interaction with R307 and/or K321 (for example, **4**) may contribute to the selective BACE inhibition.

Mapping our pharmacophore model into the BACE/cathepsin D superposed structures, two main issues can be inferred. First, it is apparent how the conserved pharmacophoric points (blue spheres in Figure 7) are essential for the ligand recognition in both the enzymes. These pharmacophoric points are placed in a region where all residues are conserved, therefore these points cannot confer selectivity.

On the contrary, some additional points (cyan spheres in Figure 7) are located in regions, which are dissimilar in BACE and cathepsin D. In particular, the H/A8 has to be considered critical for the improvement of ligand potency and selectivity by allowing the interaction with the basic triplet (N233, R235, and S325) present in BACE and not in the homologous cathepsin D. Similarly, the H6 and H7 points both offer the opportunity to obtain compounds featuring an acidic group or a H-bond acceptor on the P1′ and P2′ branches so as to allow an interaction with the R128 and K224 residues, which are only expressed in BACE.

In conclusion, despite the high sequence homology between BACE and cathepsin D, we have identified a distinctive fingerprint of the BACE catalytic site that is worth targeting in the effort to achieve potent and selective inhibitors.

## Conclusions

In the present paper an ensemble-docking approach was undertaken on six highly potent BACE inhibitors to identify plausible binding modes for each of them. A common pharmacophore model linking the multiple structural classes of inhibitors was derived. This allowed us to capture both the geometric and electronic features essential for ligand recognition and enzyme inhibition. In particular, we identified a nine point pharmacophore model outlining the relative distances among them. Interestingly, five of these points are present in all the inspected ligands; they can be referred to as essential features for ligand recognition. Whereas the other four points have been defined as accessory points of interaction. An accurate structural comparison of BACE and cathepsin D was made to support the rational design of BACE-selective inhibitors. Despite the high degree of similarity, many structural differences were identified and highlighted; these can be used to achieve or enhance selective BACE inhibition.

Both the elucidation of the binding modes of the diverse ligands and the development of an exhaustive structure-based pharmacophore model are expected to provide support for pharmacophore- and structure-based VS techniques, and a source for the optimization of screen derived hits and of established leads. Moreover, the pharmacophore hypothesis can be of help in the common target-based and ligand-based drug design approaches and for the construction of a focused-library of BACE inhibitors.

## Computational Methods

Molecular modeling calculations and graphic manipulations were performed on a Silicon Graphics Octane2 workstation equipped with two 2600 MHz R14000 processors, using the SYBYL7.2 software package.[36] Automated docking calculations were performed using version 3.0.5 of the AutoDock program.[37]

**Ligand setup:** The protonation state of ligands **1**–**6** was calculated using MarvinSketch tools (available at http://www.chemaxon.com/marvin/doc/dev/example-sketch1.1.html) at the pH value of the corresponding biological essay. The absolute stereochemistry of each ligand was considered as reported in literature. Both possible isomers of compound **2** were taken into account for the docking calculations because of the undetermined stereochemistry of the *N*-terminal hydroxyl group. For **2**, **3**, and **4** the Cambridge Structural Database (CSD)[38] was searched for the conformational preference of the cyclohexyl and the piperazinone moieties. Energy minimizations of the obtained structures were achieved with the TRIPOS force field using the SYBYL/MAXIMIN2 minimizer by applying the BFGS (Broyden, Fletcher, Goldfarb and Shannon) algorithm[39] with a convergence criterion of 0.001 kcal mol$^{-1}$. Partial atomic charges were assigned by using Gasteiger-Marsili formalism.[40] All the relevant torsion angles were treated as rotatable during the docking process, allowing a search of the conformational space.

**Protein setup:** All the X-ray structures of BACE (PDB entry codes = 1FKN, 1W51, 1TQF, 1XN3, and 2G94)[13,26–29] were set up for docking as follows: polar hydrogens were added using the BIOPOLYMERS module of the SYBYL program (the side chain of Asp 32 was taken as protonated[24,41] whereas all other Asp, Glu, Lys, and Arg side chains were considered ionized and all His were considered neutral by default), Kollman united-atom partial charges were assigned and all waters were removed. To optimize the side chain and hydrogen positions, the protein structures were minimized using both steepest descent and conjugate gradient, keeping the backbone atoms constrained by using the DISCOVER program with the CVFF force field.[42] ADDSOL utility of the AutoDock program was used to add solvation parameters to the protein structures and the grid maps representing the proteins in the docking process were calculated using AutoGrid. The grids, one for each atom type in the ligand, plus one for electrostatic interactions, were chosen to be large enough to include not only the catalytic site but also a significant part of the protein around it. As a consequence, the dimensions of grids map was 60×60×60 Å with a grid-point spacing of 0.375 Å for all docking calculations. The center of the grid was set to be coincident with one of the two oxygens of Asp 228.

  

**Docking simulation:** Docking simulations of compounds **1**–**6** were carried out using the Lamarckian Genetic Algorithm and applying a protocol with an initial population of 50 randomly placed individuals, a maximum number of $1.0\times10^6$ energy evaluations, a mutation rate of 0.02, a crossover rate of 0.80, and an elitism value of 1. Proportional selection was used, in which the average of the worst energy was calculated over a window of the previous ten generations. The pseudo-Solis and Wets algorithm with a maximum of 300 interactions was applied for the local search. 100 independent docking runs were carried out for each ligand, clustering together the resulting conformations which differ by less than 2.0 Å in positional root-mean-square deviation (rmsd). The result with the lowest free energy of binding was taken as the representative of each cluster.

**Energy refinement of the BACE-1/ligand complexes.** Energy optimizations of the obtained complexes were carried out using 3000 steps of steepest descent followed by 2000 steps of conjugated gradient algorithm employing the CVFF force field as implemented in the DISCOVER program.[42] Only the ligand and the side chains of all residues within a radius of 8 Å around the ligand were allowed to relax.

Connolly surfaces of BACE and cathepsin D were calculated using PyMOL software.[43]

**Keywords:** BACE-1 inhibitors · ensemble docking · medicinal chemistry · molecular modeling · pharmacophore model


[1] G. G. Glenner, C. W. Wong, *Biochem. Biophys. Res. Commun.* **1984**, *120*, 885 – 890.

[2] R. C. Petersen, R. G. Thomas, M. Grundman, D. Bennett, R. Doody, S. Ferris, D. Galasko, S. Jin, J. Kaye, A. Levey, E. Pfeiffer, M. Sano, C. H. van Dyck, L. J. Thal, *N. Engl. J. Med.* **2005**, *352*, 2379 – 2388.

[3] a) D. K. Lahiri, M. R. Farlow, K. Sambamurti, N. H. Greig, E. Giacobini, L. S. A. Schneider, *Curr. Drug Targets* **2003**, *4*, 97 – 112; b) M. Citron, *Neurobiol. Aging* **2002**, *23*, 1017 – 1022.

[4] R. Vassar, *Adv. Drug Delivery Rev.* **2002**, *54*, 1589 – 1602.

[5] S. Roggo, *Curr. Top. Med. Chem.* **2002**, *2*, 359 – 370.

[6] a) R. Vassar, B. D. Bennett, S. Babu-Khan, S. Kahn, E. A. Mendiaz, P. Denis, D. B. Teplow, S. Ross, P. Amarante, R. Loeloff, Y. Luo, S. Fisher, J. Fuller, S. Edenson, J. Lile, M. A. Jarosinski, A. L. Biere, E. Curran, T. Burgess, J. C. Louis, F. Collins, J. Treanor, G. Rogers, M. Citron, *Science* **1999**, *286*, 735 – 741; b) X. Lin, G. Koelsch, S. Wu, D. Downs, A. Dashti, J. Tang, *Proc. Natl. Acad. Sci. USA* **2000**, *97*, 1456 – 1460; c) S. Sinha, I. Lieberburg, *Proc. Natl. Acad. Sci. USA* **1999**, *96*, 11049 – 11053.

[7] a) D. J. Selkoe, *Nature* **1999**, *399*(6738 Suppl), A23 – A31; b) D. J. Selkoe, *Physiol. Rev.* **2001**, *81*, 741 – 766.

[8] a) H. Josien, *Curr. Opin. Drug Discov. Devel.* **2002**, *5*, 513 – 525; b) V. John, J. P. Beck, M. J. Bienkowski, S. Sinha, R. L. Heinrikson, *J. Med. Chem.* **2003**, *46*, 4625 – 4630.

[9] D. H. Small, C. A. McLean, *J. Neurochem.* **1999**, *73*, 443 – 449.

[10] Y. Luo, B. Bolon, S. Kahn, B. D. Bennett, S. Babu-Khan, P. Denis, W. Fan, H. Kha, J. Zhang, Y. Gong, L. Martin, J. C. Louis, Q. Yan, W. G. Richards, M. Citron, R. Vassar, *Nat. Neurosci.* **2001**, *4*, 231 – 232.

[11] L. A. Thompson, J. J. Brown, F. C. Zusi, *Curr. Pharm. Des.* **2005**, *11*, 3383 – 3404.

[12] M. Willem, A. N. Garratt, B. Novak, M. Citron, S. Kaufmann, A. Rittger, B. DeStrooper, P. Saftig, C. Birchmeier, C. Haass, *Science* **2006**, *314*, 664 – 666.

[13] a) M. Maillard, C. Hom, A. Gailunas, B. Jagodzinska, L. Y. Fang, J. Varghese, J. N. Freskos, S. R. Pulley, J. P. Beck, R. E. Tenbrink, WO 02/02512, **2000**b) L. Vuillard, S. Patel, J. Yon, A. Cleasby, B. Hamilton, A. Shah, WO 04/011641, **2004**; c) S. Patel, L. Vuillard, A. Cleasby, C. W. Murray, J. Yon, *J. Mol. Biol.* **2004**, *343*, 407 – 416.

[14] a) G. R. Bhisetti, J. O. Saunders, M. A. Murcko, C. A. Lepre, S. D. Britt, J. H. Come, D. D. Deninger, T. Wang, WO 02/088101, **2002**; b) D. C. Cole, E. S. Manas, J. R. Stock, J. S. Condon, L. D. Jennings, A. Aulabaugh, R. Chopra, R. Cowling, J. W. Ellingboe, K. Y. Fan, B. L. Harrison, Y. Hu, S. Jacobsen, G. Jin, L. Lin, F. E. Lovering, M. S. Malamas, M. L. Stahl, J. Strand, M. N. Sukhdeo, K. Svenson, M. J. Turner, E. Wagner, J. Wu, P. Zhou, J. Bard, *J. Med. Chem.* **2006**, *49*, 6158 – 6161.

[15] R. T. Turner III, G. Koelsch, L. Hong, P. Castenheira, A. K. Ghosh, J. Tang, *Biochemistry* **2001**, *40*, 10001 – 10006.

[16] a) B. Schmidt, H. A. Braun, R. Narlawar, *Curr. Med. Chem.* **2005**, *12*, 1677 – 1695; b) B. Schmidt, S. Baumann, H. A. Braun, G. Larbig, *Curr. Top. Med. Chem.* **2006**, *6*, 377 – 392.

[17] V. John, J. P. Beck, M. J. Bienkowski, S. Sinha, R. L. Heinrikson, *J. Med. Chem.* **2003**, *46*, 4625 – 4630.

[18] a) A. K. Ghosh, L. Hong, J. Tang, *Curr. Med. Chem.* **2002**, *9*, 1135 – 1144; b) A. K. Ghosh, D. Shin, D. Downs, G. Koelsch, X. Lin, J. Ermolieff, J. Tang, *J. Am. Chem. Soc.* **2000**, *122*, 3522 – 3523.

[19] R. K. Hom, L. Y. Fang, S. Mamo, J. S. Tung, A. C. Guinn, D. E. Walker, D. L. Davis, A. F. Gailunas, E. D. Thorsett, S. Sinha, J. E. Knops, N. E. Jewett, J. P. Anderson, V. John, *J. Med. Chem.* **2003**, *46*, 1799 – 1802.

[20] J. N. Cumming, Y. Huang, G. Li, U. Iserloh, A. Stamford, C. Strickland, J. H. Voigt, Y. Wu, J. Pan, T. Guo, D. W. Hobbs, T. X. H. Le, J. F. Lowrie, WO 05/014540, **2005**.

[21] S. J. Stachel, C. A. Coburn, T. G. Steele, M. C. Crouthamel, B. L. Pietrak, M. T. Lai, M. K. Holloway, S. K. Munshi, S. L. Graham, J. P. Vacca, *Bioorg. Med. Chem. Lett.* **2006**, *16*, 641 – 644.

[22] C. A. Coburn, S. J. Stachel, K. G. Jones, T. G. Steele, D. M. Rush, J. DiMuzio, B. L. Pietrak, M. T. Lai, Q. Huang, J. Lineberger, L. Jin, S. Munshi, M. Katharine Holloway, A. Espeseth, A. Simon, D. Hazuda, S. L. Graham, J. P. Vacca, *Bioorg. Med. Chem. Lett.* **2006**, *16*, 3635 – 3638.

[23] V. John, *Curr. Top. Med. Chem.* **2006**, *6*, 569 – 578.

[24] a) T. Polgàr, G. M. Keserü, *J. Med. Chem.* **2005**, *48*, 3749 – 3755; b) T. Polgàr, G. M. Keserü, *J. Chem. Inf. Model* **2006**, *46*, 1795 – 1805.

[25] G. B. McGaughey, D. Colussi, S. L. Graham, M. T. Lai, S. K. Munshi, P. G. Nantermet, B. Pietrak, H. A. Rajapakse, H. G. Selnick, S. R. Stauffer, M. K. Holloway, *Bioorg. Med. Chem. Lett.* **2007**, *17*, 1117 – 1121Epub.

[26] L. Hong, G. Koelsch, X. Lin, S. Wu, S. Terzyan, A. K. Ghosh, X. C. Zhang, J. Tang, *Science* **2000**, *290*, 150 – 153.

[27] C. A. Coburn, S. J. Stachel, Y. M. Li, D. M. Rush, T. G. Steele, E. Chen-Dodson, M. K. Holloway, M. Xu, Q. Huang, M. T. Lai, J. DiMuzio, M. C. Crouthamel, X. P. Shi, V. Sardana, Z. Chen, S. Munshi, L. Kuo, G. M. Makara, D. A. Annis, P. K. Tadikonda, H. M. Nash, J. P. Vacca, T. Wang, *J. Med. Chem.* **2004**, *47*, 6117 – 6119.

[28] R. T. Turner III, L. Hong, G. Koelsch, A. K. Ghosh, J. Tang, *Biochemistry* **2005**, *44*, 105 – 112.

[29] A. K. Ghosh, N. Kumaragurubaran, L. Hong, H. Lei, K. A. Hussain, C. F. Liu, T. Devasamudram, V. Weerasena, R. Turner, G. Koelsch, G. Bilcer, J. Tang, *J. Am. Chem. Soc.* **2006**, *128*, 5310 – 5311.

[30] S. F. Sousa, P. A. Fernandes, M. J. Ramos, *Proteins* **2006**, *65*, 15 – 26.

[31] a) J. N. Freskos, Y. M. Fobian, T. E. Benson, M. J. Bienkowski, D. L. Brown, T. L. Emmons, R. Heintz, A. Laborde, J. J. McDonald, B. V. Mischke, J. M. Molyneaux, J. B. Moon, P. B. Mullins, P. D. Bryan, D. J. Paddock, A. G. Tomasselli, G. Winterrowd, *Bioorg. Med. Chem. Lett.* **2007**, 17, 73-77b) J. N. Freskos, Y. M. Fobian, T. E. Benson, J. B. Moon, M. J. Bienkowski, D. L. Brown, T. L. Emmons, R. Heintz, A. Laborde, J. J. McDonald, B. V. Mischke, J. M. Molyneaux, P. B. Mullins, P. D. Bryan, D. J. Paddock, A. G. Tomasselli, G. Winterrowd, *Bioorg Med Chem. Lett.* **2007**, *17*, 78 – 81.

[32] H. A. Rajapakse, P. G. Nantermet, H. G. Selnick, S. Munshi, G. B. McGaughey, S. R. Lindsley, M. B. Young, M. T. Lai, A. S. Espeseth, X. P. Shi, D. Colussi, B. Pietrak, M. C. Crouthamel, K. Tugusheva, Q. Huang, M. Xu, A. J. Simon, L. Kuo, D. J. Hazuda, S. Graham, J. P. Vacca, *J. Med. Chem.* **2006**, *49*, 7270 – 7273.

[33] S. F. Brady, S. Singh, M. C. Crouthamel, M. K. Holloway, C. A. Coburn, V. M. Garsky, M. Bogusky, M. W. Pennington, J. P. Vacca, D. Hazuda, M. T. Lai, *Bioorg. Med. Chem. Lett.* **2004**, *14*, 601 – 604.

[34] J. Rahuel, V. Rasetti, J. Maibaum, H. Rueger, R. Goschke, N. C. Cohen, S. Stutz, F. Cumin, W. Fuhrer, J. M. Wood, M. G. Grutter, *Chem. Biol.* **2000**, *7*, 493 – 504.

[35] S. Diment, M. S. Leech, P. D. Stahl, *J. Biol. Chem.* **1988**, *263*, 6901 – 6907.


  

[36] SYBYL Molecular Modelling System, version 7.2; Tripos Inc.: St. Louis, MO, 2003.
[37] G. M. Morris, D. S. Goodsell, R. S. Halliday, R. Huey, W. E. Hart, R. K. Belew, A. J. Olson, *J. Comput. Chem.* **1998**, *19*, 1639 – 1662.
[38] F. H. Allen, S. Bellard, M. D. Brice, B. A. Cartwright, A. Doubleday, H. Higgs, T. Hummelink, B. G. Hummelink-Peters, O. Kennard, W. D. S. Motherwell, *Acta Crystallogr. Sect. B* **1979**, *35*, 2331 – 2339.
[39] J. Head, M. C. Zerner, *Chem. Phys. Lett.* **1985**, *122*, 264 – 274.
[40] J. Gasteiger, M. Marsili, *Tetrahedron* **1980**, *36*, 3219 – 3228.
[41] a) N. Moitessier, E. Therrien, S. Hanessian, *J. Med. Chem.* **2006**, *49*, 5885 – 5894; b) H. Park, S. Lee, *J. Am. Chem. Soc.* **2003**, *125*, 16416 – 16422.
[42] a) DISCOVER, Version 95.0; BIOSYM Technologies, 10065 Barnes Canyon Rd, San Diego, CA 92121; b) A. F. Hagler, S. Lifson, P. Dauber, *J. Am. Chem. Soc.* **1979**, *101*, 5122 – 5130.
[43] DeLano Scientific LLC, The PyMOL Molecular Graphics System, **2002**, http://www.pymol.org.

Received: December 21, 2006
Revised: January 30, 2007
Published online on April 3, 2007

  